Journal of Colloid and Interface Science 393 (2013) 411–420

Contents lists available at SciVerse ScienceDirect

Journal of Colloid and Interface Science

www.elsevier.com/locate/jcis

Silver/chitosan/cellulose fibers foam composites: From synthesis to antibacterial properties

Eric Guibal [a,*], Simon Cambe [a], Sandrine Bayle [b], Jean-Marie Taulemesse [c], Thierry Vincent [a]

[a] Ecole des Mines d'Alès, Laboratoire Genie de l'Environnement Industriel, Equipe Interfaces Fonctionnalisées pour l'Environnement et la Sécurité, 6, avenue de Clavières, F-30319 Alès cedex, France
[b] Ecole des Mines d'Alès, Laboratoire Genie de l'Environnement Industriel, Equipe Métrologie-Biodiagnostic, 6, avenue de Clavières, F-30319 Alès cedex, France
[c] Ecole des Mines d'Alès, Centre des Matériaux de Grande Diffusion, 6, avenue de Clavières, F-30319 Alès cedex, France

ARTICLE INFO

Article history:
Received 30 May 2012
Accepted 24 October 2012
Available online 29 November 2012

Keywords:
Silver
Chitosan
Cellulose fibers
Antibacterial
Sorption
Foams
Membranes
Antibiogram-test
Dynamic antibacterial test

ABSTRACT

Chitosan, associated with cellulose fibers, can be used for elaborating sponge-like structures (membranes, foams) for the binding of silver ions. The composite material has very promising antibacterial properties versus *Pseudomonas aeruginosa* ($Gram^-$) ≫ *Escherichia coli* ($Gram^-$) > *Staphylococcus hominis* ($Gram^+$) ≫ *Staphylococcus aureus* ($Gram^+$). The amount of silver required for bactericidal effect is quite low (below 0.1 mg per disk, this means less than 6 mg Ag g^{-1}) in antibiogram-type test but also for the treatment of water suspensions (in dynamic mode with water recycling). The presence of cellulose fibers improves the efficiency of metal binding, due to chitosan dispersion and enhancement of the availability and accessibility of amine groups. Silver nanoparticles (about 100 nm) were observed by scanning electron microscopy. The photo-reduction (exposure to sun light or UV lamp) leaded to the partial aggregation of silver nanoparticles: metal ions that were released tended to aggregate at the surface of the material.

1. Introduction

Chitosan is a biopolymer obtained by the deacetylation of chitin, one of the most abundant polysaccharide in Nature (Scheme 1). This aminopolysaccharide has found many applications in biomedical field, including wound dressing [1,2], cartilage, bone, and nerve repair [3]. One of the most interesting properties of chitin/chitosan material for biomedical applications is attributed to the hemostatic behavior of the biopolymer. Platelets are activated by chitin. In addition, the activation of macrophages with chitin/chitosan induces the controlled production of vascular endothelial growth factor [4].

Chitosan has also interesting antimicrobial properties for wound dressing applications [5] and for water disinfection [6]. The action of the chitosan depends on several characteristics such as the degree of acetylation, in relation to the cationic behavior of the polymer, the molecular weight, and its ability to bind/chelate trace metals. The p*Ka* of amino groups (which depends on the degree of acetylation) is in the range 6.4–6.7 for most commercial chitosan samples [7]. This makes the biopolymer efficient as a disinfecting agent only in acidic solutions (where amino groups are protonated, making the polymer simultaneously active and soluble). Four possibilities have been reported for improving this antimicrobial effect: (a) preparing cationic water-soluble forms of chitosan, (b) modifying chitosan by insertion of iodinated compounds [8], (c) incorporating antibiotics in the conditioned chitosan matrix [9], and (d) preparing metal–chitosan composites [10]. Several metal ions were associated with chitosan for preparing antimicrobial supports: Ag^+, Cu^{2+}, Zn^{2+}, Mn^{2+} [10]. These interactions proceed through binding on amino groups of chitosan via chelation or complexation mechanism [11]. However, the highest efficiency in disinfection was observed with silver [10,12–15]. The efficiency of silver as an antimicrobial agent has been abundantly discussed [16–26]. The broad-spectrum antimicrobial properties have already been reported in relation to biomedical applications, water and air purification, food production, cosmetics, clothing [22]. A great diversity of silver forms has been investigated: metallic silver nanoparticles, silver chloride particles, silver-impregnated zeolite or activated carbon, polymer–silver composites, bio-supports [19], such as cotton fabrics, textiles, cellulose fibers, or polysaccharides [18,20,27,28]. In particular, chitosan has retained a great attention [6,12–15,28–31]. These materials were tested for antibacterial [32–34], antifungal [35–37], and even antiviral effects [38,39]. The activity of the composite materials strongly depends on silver particle size, shape, metal

* Corresponding author. Fax: +33 (0)466782701.
E-mail address: Eric.Guibal@mines-ales.fr (E. Guibal).

0021-9797/$ - see front matter © 2012 Elsevier Inc. All rights reserved.
http://dx.doi.org/10.1016/j.jcis.2012.10.057

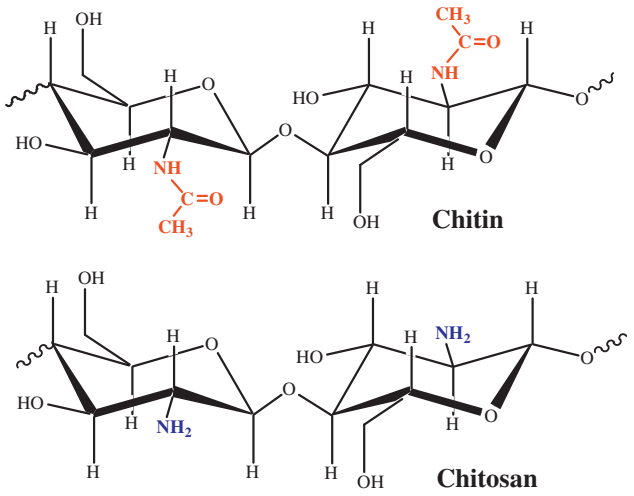

Scheme 1. Ideal structures of chitin (fully acetylated form, acetylglucosamine monomer) and chitosan (fully deacetylated form, glucosamine monomer).

environment (capping), solution pH, ionic strength, and presence of ligands [22]. The support controls the stability of silver nanoparticles as well its availability. Despite the huge number of papers dealing with silver antimicrobial effects, the mechanisms involved in the disinfection process are not fully understood. For example, in the case of antibacterial effects, the main effect of silver is supposed to be related to its release followed by (a) the uptake of free silver ions, which, in turn contribute to disrupt ATP production and DNA replication, (b) the generation of reactive oxygen species (by either silver ions or silver nanoparticles), (c) and cell membrane damage (by silver nanoparticles) [22]. However, there is a growing attention paid to the negative effects of the release of silver nanoparticles that may cause cytological damages. The release of silver is thus a great concern to be balanced between positive effect (disinfection efficiency) and negative impact (cell, organism viability). The efficiency of the silver-support composite is thus controlled by the stability of the interactions. In the solid state, the combination of silver with chitosan dressing reveals very efficient as an antimicrobial (and hemostatic) support [30,31]. Travan et al. compared the bactericidal and cytotoxic effects of a chitosan/alginate/silver composite to those of silver nanoparticles stabilized by chitosan-derivative (i.e., lactose-substituted chitosan) [28]. They show that the 3D arrangement allows decreasing the cytotoxic effect that can be observed with free silver nanoparticles. Indeed, the immobilization of the nanoparticles in the gel matrix maintains the antimicrobial activity (through a simple contact with the bacterial membrane) while preventing the nanoparticles to be undertaken and internalized by eukaryotic cells. This study confirmed the importance of chitosan conditioning on the functionalities of the biopolymer.

Chitosan is a very versatile material that can be readily modified by chemical grafting of new functional groups. It is also physically versatile. It is possible to modify the conditioning of the polymer by dissolving in an acid solution before extruding or conditioning the material under the form of gel beads [40,41], films, membranes [42–44], fibers [45,46], hollow fibers [47–49], and 3D scaffolds [50–53]. The porous properties of these materials are strongly influenced by the drying process, and it was proved that original porosity can be optimally maintained using a drying under supercritical CO_2 conditions [54,55].

The present study investigates the potential of chitosan-based supports for the immobilization of silver and the ability of the composite material for bacterial disinfection. The chitosan material is conditioned under the form of foams; cellulose fibers were added to reinforce the mechanical properties of the foams. The first part of the study deals with silver binding (sorption isotherms for different dosages of cellulose fibers). The characteristics of the composite materials are evaluated in a second step using SEM–EDAX (this part also includes the characterization of the foam under traction which is followed using the SEM). The last part of the work deals with the test of bactericidal effects. Two techniques were used for characterizing the antimicrobial efficiency of the composite materials: (a) antibiogram-type test (on a nutritive agar plate), (b) filtration mode (liquid sample pumped through the foam). The presence (and dosage) of cellulose fibers and the concentration of silver are the operative parameters considered for optimizing the synthesis of antibacterial supports. The presence of cellulose fiber is supposed to reinforce the mechanical properties of the materials and their shape stability (see Additional Material Section). Though the use of silver for improving bactericidal effect of chitosan has been previously investigated, the present sponge-like material is tested for the first time as an antimicrobial filtration system.

2. Material and methods

2.1. Material

Chitosan was supplied by Mahtani Chitosan Pvt., Ltd. (Veraval, India). The deacetylation degree, determined by FT-IR spectrometry, was 97%. Taking into account the deacetylation degree, it was possible calculating the mass of the equivalent repeating unit of the biopolymer (i.e., 162.3 g mol^{-1}). The viscosity measured by Brookfield-type viscosimeter (LVT model, 1 g of chitosan in 99 g of 1% w/w acetic acid solution) was in the range 500–2000 cPs. Cellulose fibers were prepared from an Ahlstrom raw paper substrate (Pont-Evêque, France) by dilacerations and rehydration. This is a Roburflash-type paste prepared from resinous wood (long fibers) and with poor refinery level (flash). All other reagents were analytical grade products supplied by Carlo Erba (France): The Ahlstrom raw paper was cut in small pieces (more or less 5 × 2 mm in size), before being dropped in water, and the suspension was dispersed at high velocity (1000 rpm) for 1 h. The dispersed suspension was then submitted for 15 min to IKA Ultra Turrax T-25 (about 15,000 rpm). The excess of water was removed (the percentage of dry material was determined in parallel, for the determination of appropriate amounts of cellulose fibers in the final composite materials). The dilacerations process resulted in dispersed fibrillary material. Ethanol, methanol, acetic acid (80% w/v), nitric acid (65%, w/v) and silver nitrate (0.1 M solution) were supplied by Carlo Erba (France) as reagent grade products.

Four bacteria were tested for antibacterial effects: *Escherichia coli BL21* (contaminant) obtained from Dr. Siatka (Ecole de l'ADN, D.N.A. school, France), *Staphylococcus hominis* (contaminant), *Pseudomonas aeruginosa* (pathogen) and *Staphylococcus aureus* (pathogen) obtained from Dr. Lavigne (CHU de Nîmes, University Hospital Center of Nîmes, France).

2.2. Synthesis of bactericidal supports

2.2.1. Chitosan-based supports

The biopolymers (chitosan and cellulose fibers) were pre-hydrated before use by agitation in water overnight. Chitosan particles were dissolved by adding acetic acid at the appropriate concentration (in most cases 1 g of acetic acid per gram of chitosan) in the suspension (containing cellulose fibers, at the appropriate concentration/percentage; the percentages are calculated on the basis of total mass of suspension). After complete dissolution

of the chitosan, the solution was degassed using a vacuum pump for 15 min, and the solution was left to stand for 2 h.

Different molds were used to prepare three different conditionings of composite foams: (a) rectangular plate ($117 \times 90 \times 15\ mm^3$) for plane membranes (to prepare stripes), (b) 12 wells-plate (Ø: 22 mm; height: 22 mm) for disks, and (c) perforated plate (holes: Ø: 10 mm; height: 10 mm) for cylindrical foams. The molds were lubricated with silicone oil before adding the viscous composite biopolymer suspension.

Suspension-loaded molds were stored for 1 h in a −80 °C freezer. Frozen materials were freeze-dried overnight. Dried supports were removed from molds and then coagulated in an ethanol/ammonia mixture. An appropriate amount of a 25% ammonia solution (adjusted in function of the amount of support to be coagulated on the basis of acid–base characteristics) was added to 200 mL of ethanol. The reaction took place under reflux for 1 h at the temperature of 80 °C. The supports were rinsed several times with ethanol to remove ammonia and finally dried overnight at 50 °C.

2.2.2. Silver sorption

For sorption isotherms, dried disks (weighted, m, in g) were mixed under agitation, in the dark, with a fixed volume (V; i.e., 2 mL) of silver nitrate solution at different concentrations (C_0, mg Ag L^{-1}, in the range 0–3 g L^{-1}) without controlling the pH of the solution. The molar ratios of chitosan/silver were close to 1/1, 1/0.8, 1.0.6, 1/0.4, 1/0.2, 1/0.1, 1/0.05, 1/0.025, 1/0.01, 1/0.005, 1/0.0025, and 1/ 0.00125 (Table 1) to cover a wide range of silver concentration (for detecting the impact of impregnation level on disinfection effect). After 24 h of agitation, a sample was collected for analysis using a Jobin–Yvon (Longjumeau, France) Activa-M ICP-AES (inductively-coupled plasma atomic emission spectrometer). The residual metal concentration (C_{eq}, mg Ag L^{-1}) was used for determining the sorption capacity (q, mg Ag g^{-1} disk and mg Ag g^{-1} chitosan) by the mass balance equation ($q = (C_0 - C_{eq})\text{-}V/m$). The silver-impregnated disks were then rinsed with demineralized water to remove non-sorbed metal ions. The stability of silver on the support was tested by contact of silver/biopolymer composite with a water solution, and the amount of silver released after 3 days of contact was measured by ICP-AES: this was under detection limits.

For other composite shapes, the same procedure was used for impregnating silver on membranes and cylindrical foams. The mass balance equation was used for evaluating the amount of metal bound to the polymer support.

Table 1
Amount (mg) of silver immobilized on disks (about 18 mg) tested for antibiogram-type study of bactericidal effect.

No.	Chitosan/silver mass ratio[a]		Disk reference			
			S7	S8	S9	S12
		Chitosan (%)	1	0.5	0.75	0.5
		Cell. fiber (%)	0.75	1	1	–
1	1/1		2.38	1.82	1.51	0.75
2	1/0.8		2.24	1.38	1.58	0.68
3	1/0.6		2.37	1.24	1.56	0.78
4	1/0.4		2.35	1.01	1.38	0.72
5	1/0.2		1.61	0.79	1.13	0.64
6	1/0.1		0.89	0.4	0.64	0.39
7	1/0.05		0.45	0.2	0.33	0.20
8	1/0.025		0.22	0.11	0.17	0.10
9	1/0.01		0.09	0.05	0.07	0.04
10	1/0.005		0.05	0.02	0.04	0.02
11	1/0.0025		0.02	0.01	0.02	0.01
12	1/0.00125		0.01	0.01	0.01	0.01

[a] In the silver impregnating bath.

Being silver very sensitive to light exposure, the experiments were performed in the dark. However, the precautions could not be sufficient to prevent a partial reduction of the metal, especially during the testing of bactericidal properties. When required, the silver has been reduced by irradiation for 1 h under an UV-365 nm lamp (12×2 W).

2.3. Support characterization

SEM-EDX analysis was performed on the plane membranes for observation of foam morphology and identification of metal species on specific areas of the foam. The dry sorbent was analyzed using an Environmental Scanning Electron Microscope (ESEM) Quanta FEG 200, equipped with an OXFORD Inca 350 Energy Dispersive X-ray microanalysis (EDX) system. Standard conditions for ESEM observations were set to Voltage 15 kV; Pressure 0.75 Torr, and room temperature.

A pycnometer was used to roughly evaluate the free volume of cylindrical foams; the void volume was close to 90%, using alcohol as the filling liquid to limit the swelling of the biopolymer. The suspension was passed under ultrasonic treatment for 10 min before filling the pycnometer in order to facilitate solvent diffusion.

2.4. Test of antibacterial properties

2.4.1. Petri plate inoculation

The test was carried out through the antibiogram method on agar plates. Petri dishes were prepared using a LB agar medium (composed of 10 g L^{-1} NaCl, 10 g L^{-1} tryptone, 5 g L^{-1} yeast extract and 15 g L^{-1} agar). A bacterial suspension (volume: 5 mL; initial colony-forming units, CFU: 3×10^5 bacteria mL^{-1}) was spread on the nutritive agar plate. The excess of water suspension was removed, and the agar plate was left to stand for 15 min. The dry disks (containing increasing amounts of silver, Table 1) were rehydrated with 100 μL of autoclaved demineralized water and disposed on the inoculated Petri dishes. The Petri dishes were incubated at 37 °C. After 24 h, the Petri dishes were photographed, the disks were removed, and the Petri dishes were then incubated for another 24 h-period to evaluate the type of antibacterial effect. In case of bactericidal effect, the microorganism should not grow again, while in the case of bacteriostatic effect, the bacteria can grow up again when the disk is removed.

The antibacterial effect is measured by comparison of the exclusion zone around the silver–biopolymer composite disk for the different supports: the comparison is based on the ratio of surface area exclusion zone/disk surfaces.

2.4.2. Dynamic system

In this case, the composite is used under the form of cylindrical foams inserted in a column. In order to improve the mechanical stability of the foams, they were prepared using a 1% chitosan concentration/1% cellulose fibers mixture (w/w). The amount of silver immobilized on the foam was varied. The *E. coli* bacterial suspension (volume: 100 mL; CFU: 3×10^8 bacteria mL^{-1} in 9‰ NaCl solution) was re-circulated through the column at different flow rates. At different times (first 20 drops for initial time, 1 h, 2 h, 3 h, 4 h, 5 h 30 min and 7 h), 100 μL of the suspension was collected and diluted in cascade by one order of magnitude (from 10^{-1} to 10^{-5}) and spread out with a rake on a nutritive agar plate. The inoculated agar plates were returned on the back and incubated for 24 h at 37 °C. The enumeration was then operated to evaluate the log abatement of bacteria. Experiments were duplicated and showed a deviation lower than 10%. Data will be exploited in function of (a) the operating time to evaluate the efficiency of the process and (b) the mean residence time (which represents the cumulative time of contact of the suspension with the

support, taking into account the average number of recirculation of the solution through the foam, the flow rate and the vacuum fraction in the operatory volume of the foam). Samples of the suspension were collected at the end of the experience and analyzed by ICP-AES to evaluate possible Ag release (which remained below detection limits).

3. Results and discussion

3.1. Effect of cellulose fibers on the morphology of composite materials

The introduction of cellulose fibers (CF) in the composite allows changing the properties of the material in terms of both mechanical aspects (see below), but also morphology terms. During the drying of the materials, there is a collapse of the polymer structure that causes a decrease in the size of the stripes (see Fig. AM2 in the Additional Material Section). The cellulose fibers prevent the size restriction, especially when CF and chitosan loads reach the same level. The cellulose fibers act as a reinforcing structure that partially prevents the collapse of the chitosan network. In addition, the incorporation of CF prevents the deformation of the stripes that remain plane at the highest CF load. The incorporation of CF increases the relative opacity of the material (see Fig. AM3 in the Additional Material Section). The introduction of CF also contributes to decrease the electrostatic effect of pure chitosan (see Fig. AM4 in the Additional Material Section).

3.1.1. SEM observations and SEM-EDX analysis

The incorporation of CF allows reorganizing the biopolymer network. Increasing the proportion of CF tends to qualitatively increase the opening the structure of the composite material (Fig. 1); the true porosity was not measured (preliminary measurements using BET-surface analysis were not conclusive due to the large porosity of the material).

The presence of the fibers may prevent the aggregation of the polymer chains during the drying step. The fibers of cellulose do not appear to be really embedded in the biopolymer matrix but seem to contribute to the dispersion of the biopolymer chains. It is noteworthy that the fibers were not homogeneously distributed.

The SEM-EDX analysis allows identifying the main elements present at the surface (micron-scale depth) of the samples in a fixed area (delimited *Specter i* in Fig. 2).

The first panel shows the microanalysis and the SEM photograph of the composite S4 (C1%/CF0.5%)): the main elements are those constitutive of chitosan and cellulose (i.e., C, O and N). Additionally, the SEM-EDX analysis detects the presence of Si element. The presence of traces of Si element can probably be explained by the silicone oil that was used to impregnate the molds (for facilitating the removal of foams) and that was insufficiently washed off. The second panel shows the same analysis for the sample S10 (C1%/CF1%) after Ag sorption (but without metal reduction). The sorption of the metal is appearing with small dots at the surface of the membrane on the SEM photograph. The SEM-EDX analysis

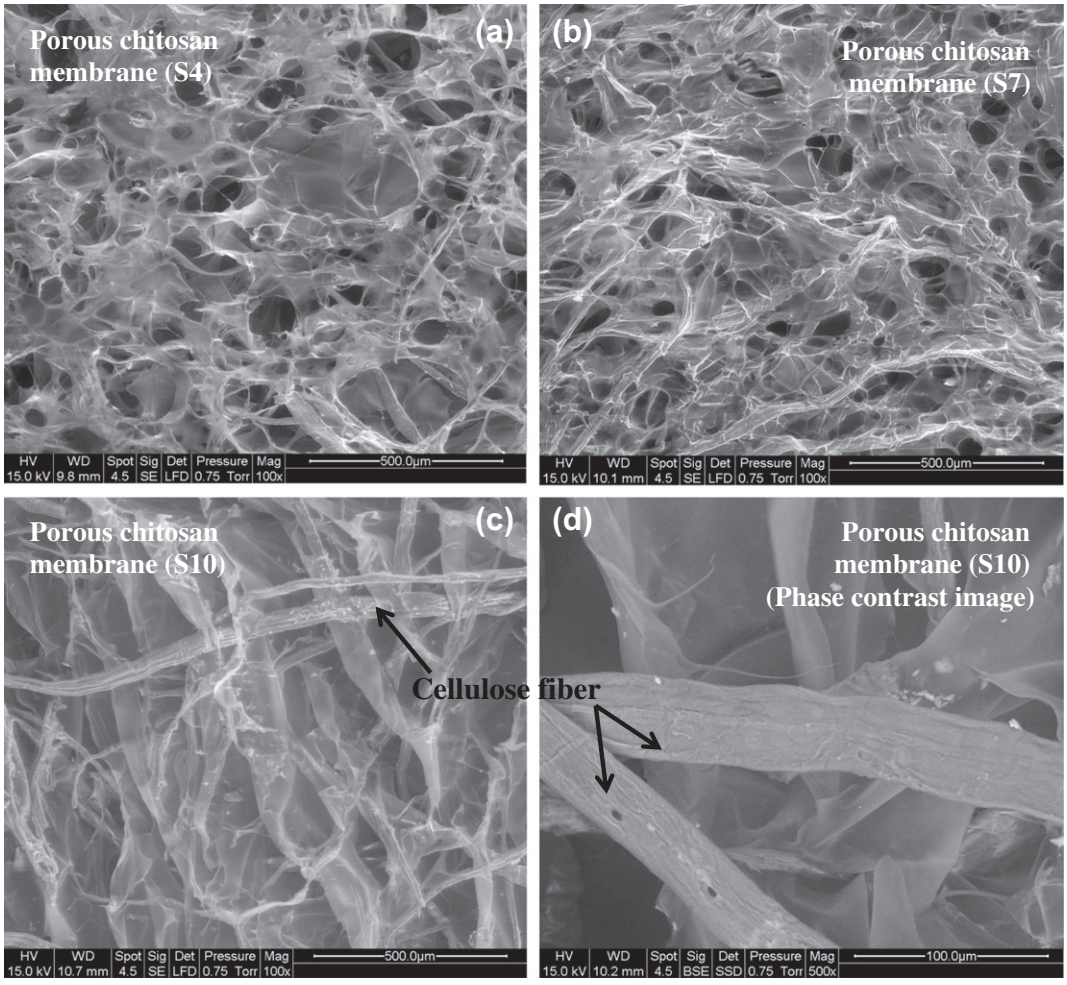

Fig. 1. SEM photograph of different lots of chitosan/cellulose fiber composites (scale bar: (a–c): 500 μm; (d): 100 μm) (S4: C1%/CF0.5%; S7: C1%/CF0.75%; S10: C1%/CF1%).

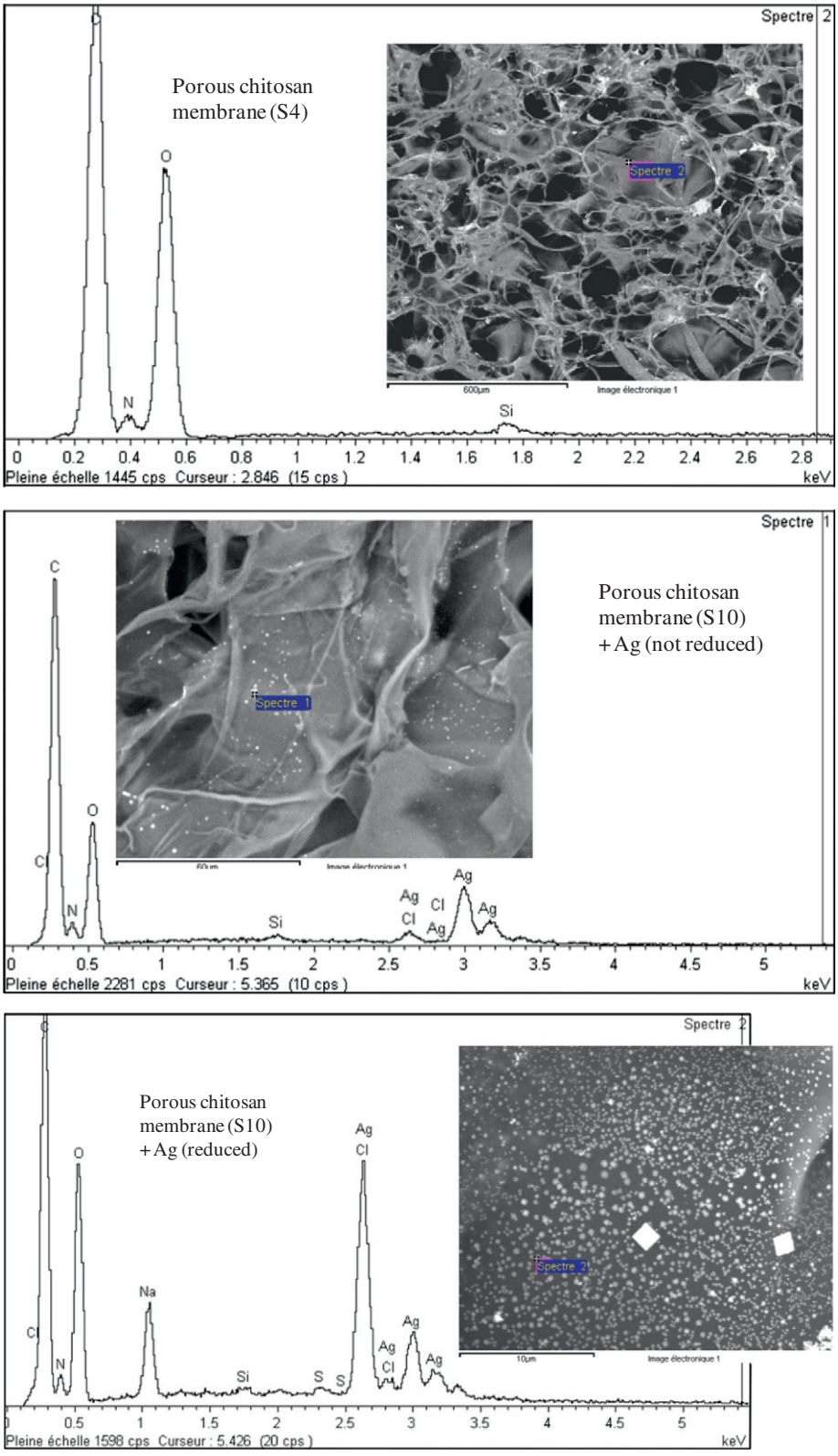

Fig. 2. SEM-EDX analyses of porous chitosan membranes at different stages of the synthesis of the silver/chitosan composite (S4: C1%/CF0.5%; S10: C1%/CF1%).

shows the presence of silver and some traces of chloride ions that remain debatable since chloride ions were not introduced in the synthesis procedure. Additionally, Cl element is superimposed with the Ag element for some rays. The last panel shows the same type of material after metal reduction.

This sample was reduced after being used for an antibacterial test (on a Petri dish): this may explain the presence of higher signals for Cl element and by the appearance of Na element (indeed, NaCl was present in the nutritive agar plate); this can be a fist explanation for the formation of large aggregates. Indeed, it is

noteworthy that silver is present under two morphological forms on the membrane (SEM photographs): small circular particles (from about 0.1 to 1 μm) and larger square particles (about 3 μm). The analysis of the square particles (see Fig. AM5 in the Additional Material Section) shows much higher bands for silver that confirm that these large crystals are silver compounds (though the area for analysis usually covers a broad space in width and height, this is sufficient here to confirm the identification). The reduction of silver by photo-irradiation may contribute to the formation of nanoparticle aggregates. During silver adsorption, the metal binding occurs through direct interaction of the metal with individual reactive groups (i.e., amine groups) without interactions between adjacently bound silver atoms. After being used and/or being reduced, there was a partial mobility of silver ions that can further aggregate (especially in the presence of chloride ions) to form these "organized" structures. Actually, the formation of these aggregates can be explained by either the photo-reduction effect or the migration/precipitation of silver in the presence of chloride anions. Similar observations were obtained with other composite membranes, and they are not reported.

3.1.2. Silver sorption

Silver sorption isotherms were established for different lots of composite materials and compared with pure chitosan support (Fig. 3). All the curves present a similar shape: (a) an initial sharp increase in the sorption capacity at low metal concentration followed by a saturation plateau. This shape is typical of Langmuir-type sorption isotherms. The experimental data can be modeled using the Langmuir equation:

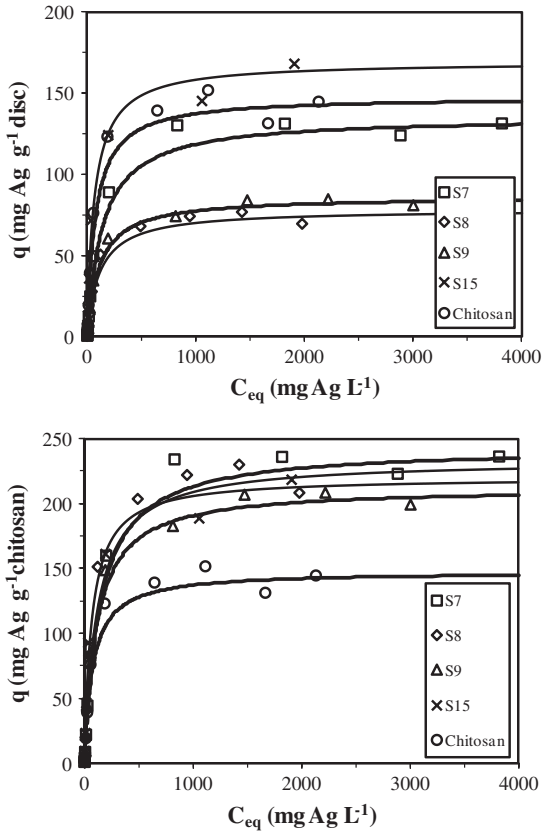

Fig. 3. Ag(I) sorption isotherms for different lots of composite chitosan/cellulose fibers disks (sorption capacity in function of disk mass: top figure; in function of chitosan mass: down figure) (S7: C1%/CF0.75%; S8: C0.5%/CF1%; S9: C0.75%/CF1%; S15: C1%/CF0.25%).

$$q = \frac{q_m b C_{eq}}{1 + b C_{eq}} \quad (1a)$$

where q_m (maximum sorption capacity at monolayer saturation; mg Ag g^{-1} or mmol Ag g^{-1}) and b (affinity coefficient; L mg^{-1} or L $mmol^{-1}$) are the parameters of the Langmuir equation. The parameters of the Langmuir equation were calculated using the linearized form:

$$C_{eq}/q = (1/(q_m b)) + (C_{eq}/q_m) \quad (1b)$$

Table 2 reports the parameters (of the Langmuir equation) for the different materials with sorption capacities reported in function of total mass of the disks and in function of chitosan mass in each disk series. Great differences are observed on sorption isotherms when the capacities are given in function of the total mass of the disks: from 75 mg Ag g^{-1} for S8 (C0.5%/CF1%) and S9 (C0.75%/CF1%) up to 120–150 mg Ag g^{-1} for 1% chitosan (with variable content of CF). Free cellulose fibers were also tested, and the sorption of silver was negligible (below 5 mg Ag g^{-1}): this means that the incorporation of CF in chitosan will directly impact the sorption capacity of the composite. However, the differences induced by the CF are not proportional to their fraction in the composite. Actually, the variation in the maximum sorption capacity is less than 15%, despite the fractions as high as 40% (of total mass). For this reason, the second panel of Fig. 3 reports the sorption isotherms as a function of chitosan amount. For composite materials, the sorption isotherms are very close and the relative proportion of CF/chitosan hardly affected sorption capacity: the maximum sorption capacity was close to 220 mg Ag g^{-1} chitosan (±10%). This is much higher than the levels reached with pure chitosan (i.e., about 140 mg Ag g^{-1} chitosan). This means that the incorporation of CF substantially improves the binding efficiency of chitosan. The cellulose fibers contribute to disperse the polymer chains that are more accessible and available for metal binding. In the absence of cellulose fibers, some interactions may exist between the different chains of the biopolymer (inter- and intra-chains) that contribute to decreasing the availability of reactive groups [56]. In order to confirm this interpretation, the maximum sorption capacity (in molar units) was compared for the different materials with their chitosan content (also on the basis of molar units of free amine groups). While for composite materials, the molar ratio was closed to 2.5 mol $-NH_2$/mole Ag in the case of free chitosan, it was close to 4 (see Fig. AM6 in the Additional Material Section). The calculation of the molar ratio $-NH_2$/Ag was based on the determination of the mass of the equivalent monomer unit of chitosan taking into account the deacetylation degree (i.e., 162.3 g mol^{-1}, see Additional Material Section). This confirms that the incorporation of CF improves the efficiency in the use of free amine groups probably by a greater dispersion of biopolymer chains. The crystallinity of the material, the interactions between the polymer chains, the conditioning of chitosan may impact the hydration of the polymer, which in turn influences the accessibility to reactive groups, and their availability for interacting with metal ions [56–58].

3.1.3. Antibiogram-type test

The inoculation of nutritive agar plates with selected bacterial strains followed by the disposal of composite silver disks allows inhibiting cell growth not only on the disk area but also on a peripheral zone, the exclusion zone (Fig. 4). In this figure (corresponding to *E. coli* inoculation and sample S8: C0.5%/CF1%), the effect of silver content on the composite material can be evaluated taking into account bacteria growth on the nutritive agar plate. The main criterion is the formation of the exclusion zone around the disk. Similar experiments were performed with silver-free disks (and silver-free cellulose fibers bands): in the absence of silver, no exclusion area was observed (Fig. AM7, see Additional

Table 2
Ag(I) sorption isotherms for different chitosan/cellulose fibers composites – parameters of the Langmuir equation.

Material	Support composition		Langmuir parameters			
	Chitosan (%)	Cellulose fibers (%)	q_m (mg Ag g^{-1} disk)	q_m (mg Ag g^{-1} chitosan)	$b \times 10^3$ (L mg^{-1})	R^2
S7	1	1	135.3 ± 2.2	243.5 ± 4.0	7.0 ± 1.2	0.997
S8	0.5	1	77.8 ± 4.0	233.4 ± 11.9	8.4 ± 3.0	0.975
S9	0.75	1	86.1 ± 1.4	212.5 ± 3.4	8.8 ± 1.5	0.998
S15	1	0.25	169.1 ± 4.2	219.8 ± 5.4	14.2 ± 3.3	0.996
Chitosan	1	0	147.7 ± 3.6	147.7 ± 3.6	13.0 ± 3.3	0.994

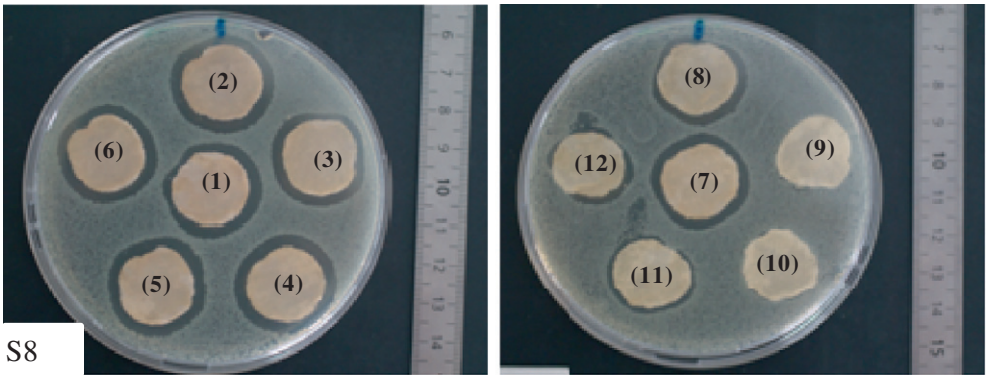

Fig. 4. Antibiogram-type results for *E. coli* (0.5% chitosan/1% cellulose fiber, reference sample S8 (C0.5%/CF1%); 1–12: decreasing amounts of silver – Table 2).

Material Section). But, it is noteworthy that the no bacterial development was observed under the disks. The antibacterial effect of chitosan and cellulose fibers (without silver sorption) was shown by the absence of growth after removing the disks from the plate. The absence of growth for chitosan-based composites (after being re-incubated) shows that the biopolymer has an antibacterial effect (and not a bacteriostatic effect as in the case of growing bacteria).

For the samples 1–7 (this means a silver content in the range 0.2–1.82 mg per disk, Table 1 in the Additional Material Section), the exclusion zone hardly varied with silver content, for lower Ag-content, the exclusion zone tended to decrease and to become negligible. Similar studies were performed with different composites (samples S7 (C1%/CF0.75%), S9 (C0.75%/CF1%) and S12 (C0.5%/CF0%)) and with different bacterial strains (*S. hominis*, *S. aureus* and *P. aeruginosa*). Fig. 5 compares for both *E. coli* and *S. hominis* the evolution of the exclusion zone (as the surface area ratio between the exclusion zone and the surface area of the disk used for given experiments). For *E. coli*, the surface area ratio (SAR) increased with the amount of silver immobilized on the disk. When the amount of silver exceeds 0.4–0.6 mg (per disk), the efficiency of the antibacterial effect no more increased and tended to stabilize. For *S. hominis,* the SAR also increased with metal content; however, for most of the tested samples, the SAR slowly increased even above 0.4–0.6 mg Ag-content contrary to *E. coli* (for which, there was a stabilization of the bactericidal effect). In addition, it is possible to observe that the surface area for the exclusion zone was systematically lower for *S. hominis* than for *E. coli*. The size of the exclusion zone was systematically higher for disks made of pure chitosan than those of the composite materials. The size of chitosan disks was much lower than that of chitosan/CF because the presence of cellulose fibers increases the mechanical stability of the disks and limits the collapse of the porous structure. This means also that the active surface surrounding the disk (corresponding to silver action) represents in proportion a greater fraction of the disk surface than with composite materials. This is probably one of the reasons that can explain the higher SAR.

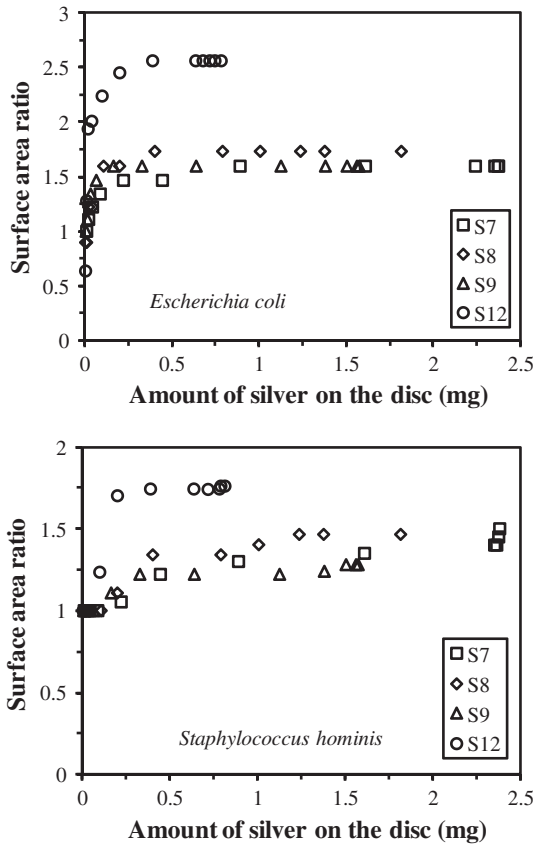

Fig. 5. Influence of silver loading on the antibacterial effect (SAR) of Ag/chitosan/cellulose fiber composites against *E. coli* and *S. hominis* for different supports (S7: C1%/CF0.75%; S8: C0.5%/CF1%; S9: C0.75%/CF1%; S12: C0.5%/CF0%).

In the case of *S. aureus* (pathogenic bacteria), the exclusion area surrounding the disk was much thinner than for *E. coli* and *S. hominis*. Additionally, the amount of silver required slightly increased

compared to other strains. This means that *S. aureus* was probably less sensitive to silver nanoparticle than the other bacteria. The case of *P. aeruginosa* (pathogen bacteria) is substantially different. Indeed, Fig. AM8 (see Additional Material Section) shows that a very large exclusion zone appears around the disks. In the case of the higher silver charges (samples 1–5; i.e., 0.8–1.8 mg per disk), only a very limited central area was colonized.

The exclusion area was much larger than those found with *E. coli*, and *S. aureus*. In addition, the amount of silver needed for detecting an appreciable limitation of bacteria growth (i.e., about 0.1 mg) is lower than for *E. coli*, for example. *P. aeruginosa* appears to be significantly more sensitive to silver than other bacteria strains.

The comparison of antibiogram tests for sample S8 (C0.5%/CF1%) (Fig. 6) shows that the efficiency of the silver composites follows the series:

$$P.\ aeruginosa\ (\mathrm{Gram}^-) \gg E.\ coli\ (\mathrm{Gram}^-) > S.\ hominis\ (\mathrm{Gram}^+) \gg S.\ aureus\ (\mathrm{Gram}^+).$$

The bactericidal effect of the composite disk can be correlated to the minimum inhibitory concentration (MIC) of silver for these different strains.

The mechanism of silver ion (Ag^+) action may be attributed to the sorption of silver ions on biological molecules inside the bacterial cells: they bind on dithioketal moieties of the cellular proteins and enzymes [22]. They also replace metal ions in enzyme prosthetic groups causing the disruption of the enzyme structure and the inhibition of its proper functions. They can also bind to natural DNA. The Ag–DNA complexes displace hydrogen bonds between adjacent nitrogen of purines and pyrimidines causing the denaturation of DNA and RNA and preventing replication. Additionally, silver nanoparticles, when released from the support (or directly present in the suspension, depending on the mode of administration of the antibacterial agent), may contribute to generate reactive oxygen species but also to directly damage the cell wall [22].

The exclusion zone observed on the antibiogram tests could indicate that a fraction of silver was released from the disks, due to the affinity of silver for agar plate and the presence of salt in the gelose, the metal was mobilized and migrated at the surface of the plate. In the case of dynamic tests (see below), the effect of possible silver release is minimized by the recirculation of the solution and the great affinity of silver for chitosan (metal binding to amine groups of chitosan by chelation). This could explain that the concentration of silver in the solution remains negligible.

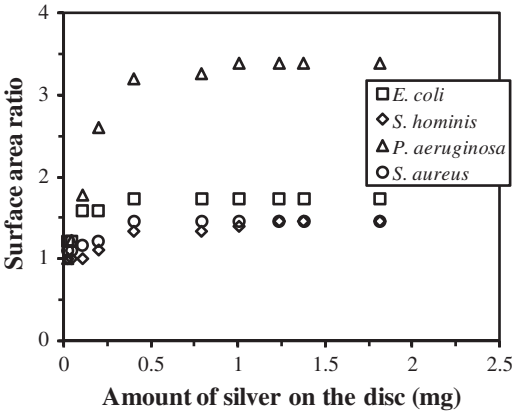

Fig. 6. Influence of silver loading on the antibacterial effect (SAR) of Ag/chitosan/cellulose fiber composites against *E. coli*, *S. hominis*, *S. aureus*, and *P. aeruginosa* (sample: S8: C0.5%/CF1%).

The state of silver on the disks was not fully characterized. Though the synthesis was as far as possible performed in the dark to prevent the reduction of silver ions, it is not possible to reject the hypothesis of, at least, a partial reduction of the metal. Complementary experiments were performed with composite materials that were subjected to photo-reduction. The treatment was followed by a darkening of the disks that proves the reduction in the metal. Antibacterial tests were performed using the same experimental procedure on reduced-Ag disks (those containing the lowest amounts of silver, that is, samples S7–S12, see Table 1). It was not possible detecting significant differences in the antibacterial efficiency after silver was photo-reduced (see an example in Fig. AM9, in the Additional Material Section). This section shows that the oxidation state of silver (reduced or not) on the composite materials had a little effect on their antibacterial property.

3.1.4. Antibacterial effect in column system

In order to verify the bactericidal effect of chitosan–silver composite materials in a different mode of application, complementary tests were performed in liquid systems using the composite material under the form of cylindrical foams immobilized in a column. The bacterial suspension (*E. coli* in 9‰ NaCl solution) was pumped up-flow through the loaded column. The solution was recycled, and samples were regularly collected for colony counting on a LB nutritive agar plate. The foams were prepared with the composition corresponding to sample S10 (C1%/CF1%) loaded with 3.1 mg of silver (mass of the foam: 17 mg; apparent volume: 0.265 mL; void percentage: 90%). The flow rate was varied between

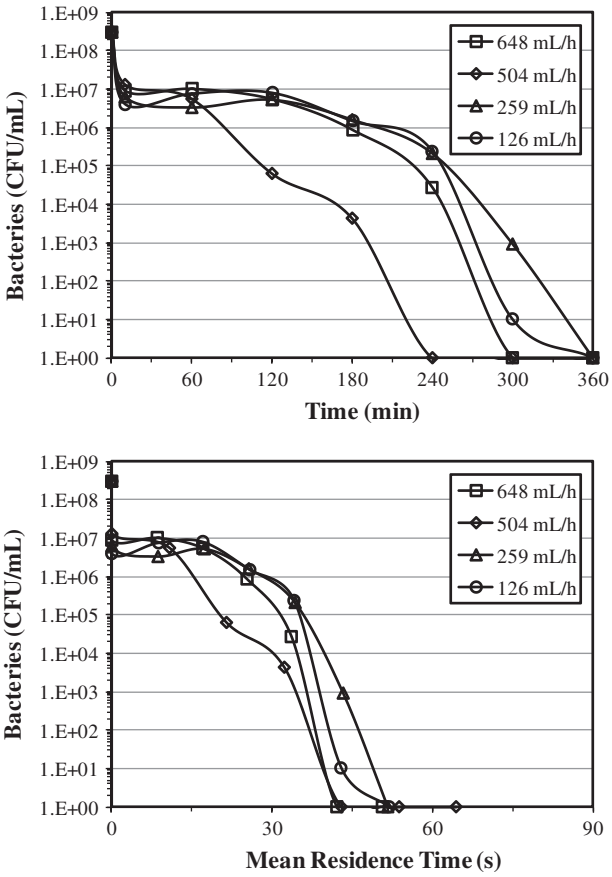

Fig. 7. Antibacterial effect in dynamic mode using composite Ag/chitosan/cellulose fibers foams – influence of flow rate on the abatement of *E. coli* colony number (CFU/mL): plots in function of time and mean residence time (S10: C1%/CF1%; mass of foam: 17 mg; silver amount 3.1 mg).

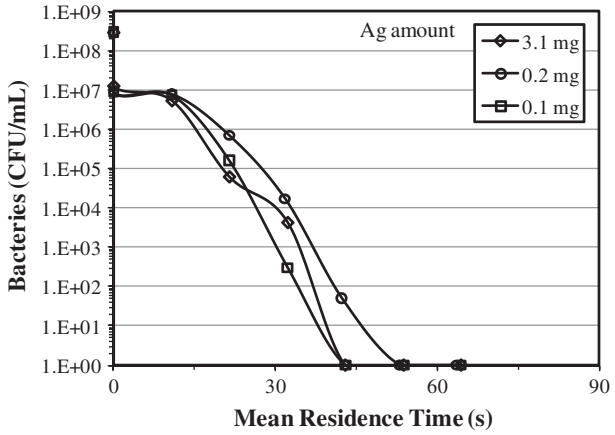

Fig. 8. Antibacterial effect in dynamic mode using composite Ag/chitosan/cellulose fibers foams – influence of silver amount on the abatement of *Escherichia coli* colony number (CFU/mL): plots in mean residence time (S10: C1%/CF1%; mass of foam: 17 mg).

126 mL h^{-1} and 648 mL h^{-1}. This corresponds to mean residence times (in a single cycle) between 1.3 and 7 s. The cumulative residence time will be calculated as the mean residence time (at fixed flow rate) multiplied by the number of cycles (total volume of the suspension divided by the flow rate reported to operating time) through the foam for target contact time. The colony-forming units per mL (CFU) were plotted in function of time and mean residence time (i.e., cumulative residence time) in Fig. 7. The figure shows that (a) the flow rate had a limited impact on the abatement of bacterial population; (b) it is possible to reach a 7/8-log abatement of the population within 4–6 h of operating time. Logically, increasing the flow rate required a greater number of cycles to reach the target level of bacteria abatement because it decreases the time passed in the foam (Fig. AM10, Additional Material Section). The number of cycles varied between 8 and 32 with increasing flow rate. The cumulative residence time required for complete disinfection varied between 40 and 55 s. On the second panel of Fig. 7, it appears that the impact of flow rate is limited when the bacteria abatement is plotted versus cumulative residence time: an effective contact time of 1 min reveals sufficient to reach the target abatement. It is noteworthy that all the curves begin with a lag-phase corresponding to about 10 min for which the bacteria abatement was limited to one log-unit.

This lag-phase can probably be explained by the huge porosity of the foam (several dozens of micrometer favorable for water permeation) that makes the formation of preferential channels. As a consequence, the bacteria cells may pass through the foam without being in contact with silver nanoparticles. Several passes may be necessary for making detectable inactivation of the bacterial load.

Complementary experiments were performed with the same support changing silver loading: the amount of silver bound to the support was decreased to 0.2 and 0.1 mg (Fig. 8). The figure clearly shows that even at the lowest silver loading (i.e., 0.1 mg), the bacteria abatement was comparable to the levels reached with a charge of 3.1 mg (for 17 mg of chitosan/CF composite foam. Similar profiles were observed when plotting bacteria abatement in function of operating time and number of cycles (not shown).

4. Conclusion

The immobilization of silver on chitosan foams allows manufacturing very efficient antibacterial supports that were demonstrated on both antibiogram-type tests (on nutritive agar plates) and in dynamic tests (aqueous suspension). The amount of silver to be immobilized is quite low (as low as 6 mg Ag g^{-1} on foams) for achieving a 7/8-log abatement level on *E. coli*. In antibiogram-type tests, the efficiency of the composite material was also demonstrated on other bacteria such as *P. aeruginosa*, *S. hominis* and to a lesser extent to *S. aureus*. The inclusion of cellulose fibers in the composite material brings interesting mechanical properties preventing the collapse of the structure of the conditioned polymer (size, morphology). Additionally, the presence of cellulose fibers enhances the dispersion of the biopolymer and the sorption properties of the composite chitosan/cellulose fibers for silver are significantly improved (when compared on the basis of chitosan amount) since the amine groups become more accessible and/or available. The release of silver from the support was not detected in the suspension (below detection limits) though it cannot be rejected: this can be explained by the affinity of silver for chitosan (metal chelation). The oxidation state of the metal (and more generally the metal speciation) is a key parameter for the understanding of the mechanisms involved in the antibacterial effect of these materials (and the evaluation of their efficiency). Appropriate analytical tools (such as XPS) were not available for the determination of the oxidation state of silver at the different stages of the use of these materials. However, as previously indicated, the UV irradiation of the antimicrobial supports (using an UV lamp) changed the color of the disks (darkened, as en evidence of metal reduction at the surface of the biopolymer) without changing the antimicrobial activity.

The combination of hemostatic properties of chitosan and its sorption properties (for Ag(I)) allows synthesizing a very promising support for biomedical applications (providing the release of silver ions or silver nanoparticles could be prevented or controlled). However, the conditioning of the support under the form of very-opened foams opens also the route for applications in the field of water disinfection in crisis environment (securing water supply). The potential of these materials will be evaluated in the future for long-lasting use in order to better define the application field of these materials.

Acknowledgment

Mahtani Chitosan Pvt., Ltd. (Veraval, India) is acknowledged for the gift of chitosan samples.

Appendix A. Supplementary material

Supplementary data associated with this article can be found, in the online version, at http://dx.doi.org/10.1016/j.jcis.2012.10.057.

References

[1] M.A. Brown, M.R. Daya, J.A. Worley, J. Emerge. Med. 37 (2009) 1.
[2] C. Alemdaroglu, Z. Degim, N. Çelebi, F. Zor, S. Öztürk, D. Erdogan, Burns 32 (2006) 319.
[3] R.A.A. Muzzarelli, Carbohydr. Polym. 76 (2009) 167.
[4] R.L. Gu, W.H. Sun, H. Zhou, Z.N. Wu, Z.Y. Meng, X.X. Zhu, Q. Tang, J. Dong, G.F. Dou, Biomaterials 31 (2010) 1270.
[5] T.H. Dai, G.P. Tegos, M. Burkatovskaya, A.P. Castano, M.R. Hamblin, Antimicrob. Agents Chemother. 53 (2009) 393.
[6] Q. Li, S. Mahendra, D.Y. Lyon, L. Brunet, M.V. Liga, D. Li, P.J.J. Alvarez, Water Res. 42 (2008) 4591.
[7] P. Sorlier, A. Denuzière, C. Viton, A. Domard, Biomacromolecules 2 (2001) 765.
[8] M. Banerjee, S. Mallick, A. Paul, A. Chattopadhyay, S.S. Ghosh, Langmuir 26 (2010) 5901.
[9] F.-L. Mi, Y.-B. Wu, S.-S. Shyu, J.-Y. Schoung, Y.-B. Huang, Y.-H. Tsai, J.-Y. Hao, J. Biomed. Mater. Res. 59 (2002) 438.
[10] W.-L. Du, S.-S. Niu, Y.-L. Xu, Z.-R. Xu, C.-L. Fan, Carbohydr. Polym. 75 (2009) 385.
[11] E. Guibal, Sep. Purif. Technol. 38 (2004) 43.
[12] D.V. Phu, V.T.K. Lang, N.T. Kim Lan, N.N. Duy, N.D. Chau, B.D. Du, N.Q. Hien, J. Exp. Nanosci. 5 (2010) 169.
[13] R. Yoksan, S. Chirachanchai, Mater. Chem. Phys. 115 (2009) 296.
[14] R. Yoksan, S. Chirachanchai, Mater. Sci. Eng., C 30 (2010) 891.

[15] Y. Qin, C. Zhu, J. Chen, J. Zhong, J. Appl. Polym. Sci. 104 (2007) 3622.
[16] J.S. Kim, E. Kuk, K.N. Yu, J.H. Kim, S.J. Park, H.J. Lee, S.H. Kim, Y.K. Park, Y.H. Park, C.Y. Hwang, Y.K. Kim, Y.S. Lee, D.H. Jeong, M.H. Cho, Nanomed. Nanotechnol. Biol. Med. 3 (2007) 95.
[17] A. Fernandez, E. Soriano, G. Lopez-Carballo, P. Picouet, E. Lloret, R. Gavara, P. Hernandez-Munoz, Food Res. Int. 42 (2009) 1105.
[18] V. Ilic, Z. Saponjic, V. Vodnik, B. Potkonjak, P. Jovancic, J. Nedeljkovic, M. Radetic, Carbohydr. Polym. 78 (2009) 564.
[19] V.K. Sharma, R.A. Yngard, Y. Lin, Adv. Colloid Interface Sci. 145 (2009) 83.
[20] E. Chadeau, N. Oulahal, L. Dubost, F. Favergeon, P. Degraeve, Food Control 21 (2010) 505.
[21] L. Chen, L. Zheng, Y. Lv, H. Liu, G. Wang, L.N.R. Duo, J. Wang, R.I. Boughton, Surf. Coat. Technol. 204 (2010) 3871.
[22] C. Marambio-Jones, E.M.V. Hoek, J. Nanopart. Res. 12 (2010) 1531.
[23] F. Martinez-Gutierrez, P.L. Olive, A. Banuelos, E. Orrantia, N. Nino, E.M. Sanchez, F. Ruiz, H. Bach, Y. Av-Gay, Nanomed. Nanotechnol. Biol. Med. 6 (2010) 681.
[24] X. Zan, Z. Su, Thin Solid Films 518 (2010) 5478.
[25] M. Sureshkumar, D.Y. Siswanto, C.K. Lee, J. Mater. Chem. 20 (2010) 6948.
[26] Y.M. Ye, Q. Song, Y. Mao, J. Mater. Chem. 21 (2011) 257.
[27] D. Klemencic, B. Simoncic, B. Tomsic, B. Orel, Carbohydr. Polym. 80 (2010) 426.
[28] A. Travan, C. Pelillo, I. Donati, E. Marsich, M. Benincasa, T. Scarpa, S. Semeraro, G. Turco, R. Gennaro, S. Paoletti, Biomacromolecules 10 (2009) 1429.
[29] F.-L. Mi, Y.-B. Wu, S.-S. Shyu, A.-C. Chao, J.-Y. Lai, C.-C. Su, J. Membr. Sci. 212 (2003) 237.
[30] M. Burkatovskaya, G.P. Tegos, E. Swietlik, T.N. Demidova, A.P. Castano, M.R. Hamblin, Biomaterials 27 (2006) 4157.
[31] S.-Y. Ong, J. Wu, S.M. Moochhala, M.-H. Tan, J. Lu, Biomaterials 29 (2008) 4323.
[32] A. Dror-Ehre, H. Mamane, T. Belenkova, G. Markovich, A. Adin, J. Colloid Interface Sci. 339 (2009) 521.
[33] L.F. Espinosa-Cristóbal, G.A. Martínez-Castañón, R.E. Martínez-Martínez, J.P. Loyola-Rodríguez, N. Patiño-Marín, J.F. Reyes-Macías, F. Ruiz, Mater. Lett. 63 (2009) 2603.
[34] H. Miyoshi, H. Ohno, K. Sakai, N. Okamura, H. Kourai, J. Colloid Interface Sci. 345 (2010) 433.
[35] Y.K. Jo, B.H. Kim, G. Jung, Plant Dis. 93 (2009) 1037.
[36] S.D. Gittard, D. Hojo, G.K. Hyde, G. Scarel, R.J. Narayan, G.N. Parsons, J. Mater. Eng. Perform. 19 (2010) 368.
[37] A. Panácek, M. Kolár, R. Vecerová, R. Prucek, J. Soukupová, V. Krystof, P. Hamal, R. Zboril, L. Kvítek, Biomaterials 30 (2009) 6333.
[38] L. Lu, R.W.Y. Sun, R. Chen, C.K. Hui, C.M. Ho, J.M. Luk, G.K.K. Lau, C.M. Che, Antiviral Ther. 13 (2008) 253.
[39] K. Zodrow, L. Brunet, S. Mahendra, D. Li, A. Zhang, Q.L. Li, P.J.J. Alvarez, Water Res. 43 (2009) 715.
[40] E. Guibal, C. Milot, O. Eterradossi, C. Gauffier, A. Domard, Int. J. Biol. Macromol. 24 (1999) 49.
[41] D. Sicupira, K. Campos, T. Vincent, V. Leao, E. Guibal, Adsorption 16 (2010) 127.
[42] Z. Modrzejewska, W. Kaminski, Ind. Eng. Chem. Res. 38 (1999) 4946.
[43] M.M. Beppu, R.S. Vieira, C.G. Aimoli, C.C. Santana, J. Membr. Sci. 301 (2007) 126.
[44] R.S. Vieira, E. Guibal, E.A. Silva, M.M. Beppu, Adsorption 13 (2007) 603.
[45] Q.C. Agboh, Y. Qin, Polym. Adv. Technol. 8 (1997) 355.
[46] W. Kaminski, W. Eckstein, Z. Modrzejewska, Z. Sroda, in: Z.S. Karnicki, A. Wojtasz-Pajak, M.M. Brzeski, P.J. Bykowski (Eds.), Chitin World, Wirtschaftsverlag NW, Bremerhaven, Germany, 1995, p. 600.
[47] T. Vincent, E. Guibal, Environ. Sci. Technol. 38 (2004) 4233.
[48] T. Vincent, E. Guibal, Ind. Eng. Chem. Res. 40 (2001) 1406.
[49] F. Peirano, T. Vincent, E. Guibal, J. Appl. Polym. Sci. 107 (2008) 3568.
[50] S.V. Madihally, H.W.T. Matthew, Biomaterials 20 (1999) 1133.
[51] H.J. Chun, G.W. Kim, C.H. Kim, J. Phys. Chem. Solids 69 (2008) 1573.
[52] H.R. Lin, K.S. Chen, S.C. Chen, C.H. Lee, S.H. Chiou, T.L. Chang, T.H. Wu, Mater. Sci. Eng., C 27 (2007) 280.
[53] Y. Shirosaki, T. Okayama, K. Tsuru, S. Hayakawa, A. Osaka, Chem. Eng. J. 137 (2008) 122.
[54] R. Valentin, B. Bonelli, E. Garrone, F. Di Renzo, F. Quignard, Biomacromolecules 8 (2007) 3646.
[55] R. Valentin, K. Molvinger, F. Quignard, D. Brunel, New J. Chem. 27 (2003) 1690.
[56] E. Piron, M. Accominotti, A. Domard, Langmuir 13 (1997) 1653.
[57] E. Piron, A. Domard, Int. J. Biol. Macromol. 21 (1997) 327.
[58] E. Guibal, E. Touraud, J. Roussy, World J. Microbiol. Biotechnol. 21 (2005) 913.